Nuclear Exclusive and Semi-inclusive Physics with a New CLAS12 Low Energy Recoil Detector

K. Hafidi[†‡], J. Arrington, D.F. Geesaman, R. J. Holt, A. El Alaoui[†], R. Dupré[†], B. Mustapha, D. H. Potterveld, P. E. Reimer

Argonne National Laboratory, Argonne IL 60439, USA

L. Zhu[†]

Hampton University, Hampton, VA 23668, USA

S. Dhamija

Florida International University, Miami, Fl 33199, USA

A. Accardi[1], V. Burkert, D. Gaskell[†], F.-X. Girod[†], V. Guzey, H. Fenker, V. Kubarovsky, S. Stepanyan[†]

Jefferson Laboratory, Newport News, VA 23606, USA

D. Dutta[†]

Mississippi State University, Mississippi State, USA

C. Salgado

Norfolk State University, Norfolk, VA 23504, USA

S. Danagoulian

North Carolina A&T State University, NC 27411, USA

A. Daniel

Ohio University, Athens, OH 45701, USA

M. Amarian[†], S. Bueltmann, G. Gavalian, S. Kuhn, L. Weinstein

Old Dominion University, Norfolk, VA 23529, USA

JLab Letter of Intent to PAC35 *14 December 2009*

L. El Fassi

Rutgers University, Piscataway, NJ 08854, USA

H. Egiyan[†], M. Holtrop, L. Zana

University of New Hampshire, Durham, NH 03824, USA

W. Brooks[†]

Universidad Técnica Federico Santa María, Valparaíso, Chile

G.P. Gilfoyle[†]

University of Richmond, Richmond, VA 23173, USA

S. Liuti[†]

University of Virginia, Charlottesville, VA 22904-4714, USA

C. Ciofi degli Atti, C. B. Mezzetti, S. Scopetta

University of Perugia and INFN Sezione di Perugia, Perugia, Italy

L. P. Kaptari

Bogoliubov Lab. of Theoretical Physics, JINR, Dubna, Russia

---

[1] and Hampton University, Hampton, VA

[†] Spokesperson

[‡] Contact person, kawtar@anl.gov

Abstract

The 11 GeV beam of the upgraded Jefferson Lab combined with the CLAS12 detector provides a unique opportunity to investigate the internal structure of nuclei and to understand the effect of the nuclear matter on the structure of hadrons. It also allows us to study the properties of QCD by measuring the internal structure of hadrons themselves and by studying the spectrum of the QCD bound states. Many of the processes needed to research these subjects require the detection of a low momentum recoil particle in the final state, which may often be an experimental challenge. We intend to perform a set of different experiments on proton and nuclear targets with 11 GeV electron beam and the CLAS12 detector in Hall B. All of the considered experiments will also require an additional specialized detector for low energy recoil fragments. In this Letter of intent we briefly describe the physics objectives of these experiments, and suggest different options for a recoil detector optimized for all the described measurements.

Contents

1 Introduction

In this letter we are presenting a broad physics program. It covers the study of the hadron structure, meson spectroscopy and next generation nuclear chromodynamics measurements. For this program to be successful, it is crucial to be able to tag low energy recoil spectators.

We propose to investigate several low energy recoil detector options for CLAS12. This device will be able to detect low energy recoiling protons and nuclei. In the next section, details about the physics program are presented. We plan later to develop each physics topic into an independent proposal. However, there is a consensus among the authors of this letter that simulation, design, and construction of such a device should be coordinated among all participating institutions to ensure that the detector is optimized for all the physics discussed here.

2 Physics Topics

2.1 Coherent and incoherent DVCS on helium

During the last decade, Deeply Virtual Compton Scattering (DVCS) has emerged as a powerful tool to investigate the quark and gluon structure of hadronic matter [1–3]. The scattering of energetic photons off the nucleus in the Bjorken regime tells us about the momentum and position distributions of the quarks and the gluons. These features are described within the recent GPD formalism [4] which provides a comprehensive picture of the structure of hadrons. GPDs correspond to the coherence between quantum states of different (or same) helicity, longitudinal momentum, and transverse position. In an impact parameter space they can be interpreted as distributions in the transverse plane of partons carrying a certain longitudinal momentum [5–7]. A crucial feature of GPDs is the access to the transverse position of partons which, combined with their longitudinal momentum, leads to the total angular momentum of partons [8]. This information is inaccessible to inclusive deep inelastic scattering (DIS) which measures probability amplitudes in the longitudinal plane. DVCS, (see Fig. 1) corresponding to the absorption of a virtual photon by a quark followed quasi-instantaneously by the emission of a real photon, is the simplest process to access GPDs. In addition to the DVCS amplitude, the cross section for electroproduction of photons ($eN \rightarrow eN\gamma$) gets also contributions from the Bethe-Heitler (BH) process where the real photon is emitted either by the initial or the final lepton. The reaction amplitude $|\mathcal{T}|^2$

is the coherent sum of the terms of the BH and DVCS amplitudes, therefore:

$$|\mathcal{T}|^2 = |\mathcal{T}_{\rm BH}|^2 + |\mathcal{T}_{\rm DVCS}|^2 + \mathcal{I}, \tag{1}$$

where $\mathcal{I}$ being the interference between BH and DVCS amplitudes.

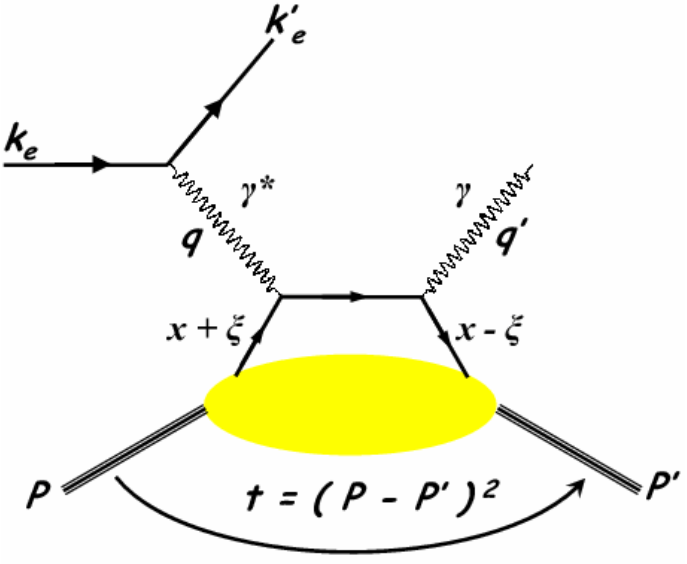

Fig. 1. The handbag diagram corresponding to DVCS. In the handbag diagram, $x + \xi$ ($x - \xi$) refers to the longitudinal momentum fraction of the initial (final) quark, and $t = (P - P')^2$ is the squared momentum transfer between the initial t and the recoiled target.

The spin zero of certain stable nuclei such as the helium, xenon or neon allows for a simple parametrization of its partonic structure characterized at leading twist by one chirally-even GPD H_A, which greatly simplifies the analysis process to extract the individual GPDs. In the forward limit ($t \to 0$), this GPD reduces to the usual parton densities of the spin-0 nucleus measured in DIS. In addition, a number of interesting relationships were found by studying Mellin moments in nuclei: the A-dependence for the D-term of GPDs was estimated within microscopic approaches [9,10], and compared with the calculation of Ref. [11] using a liquid drop model; a connection was made in Ref. [9] with the widely used approaches that relate the modifications of "partonic" parameters such as the string tension, or the confinement radius, to density dependent effects in the nuclear medium (see Ref. [12] and references therein).

The results from the recent DVCS experiments at the Jefferson Laboratory (JLab) [13,14] are consistent with the dominance of the handbag diagram in the description of the DVCS process on the nucleon. It is the goal of this letter to employ the DVCS reaction in the coherent and incoherent channels for the investigation of the internal structure of the ^{4}He nucleus. The main emphasis of this experiment is the measurement of the Beam-Spin asymmetry (BSA) of

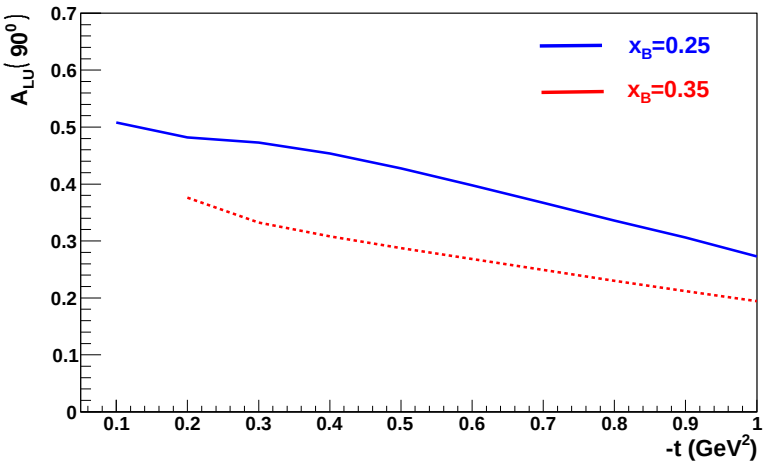

Fig. 2. Beam spin asymmetry versus momentum transfer $-t$ at x_B=0.25 (solid curve) and x_B=0.35 (dashed curve) from the model by Guzey and Strikman [15] calculated for coherent DVCS on ^{4}He target at electron beam energy of 11 GeV.

the DVCS process which allows us to access the imaginary as well as the real parts of the Compton form factor of the single GPD of the helium nucleus. Figure 2 shows predictions from the model by Guzey and Strikman [15] for DVCS beam spin asymmetry at $\phi = 90^0$ versus four-momentum transfer t. For a scalar target, the beam-spin asymmetry can be expressed as [16]:

$$A_{LU} = \frac{\alpha_0(\phi)\Im_A}{\alpha_1(\phi) + \alpha_2(\phi)\Re_A + \alpha_3(\phi)(\Re_A^2 + \Im_A^2)} \ , \tag{2}$$

where $\Im_A = \Im m\{\mathcal{H}_A\}$, $\Re_A = \Re e\{\mathcal{H}_A\}$ are the unknown imaginary and real parts of the Compton form factor and the $\alpha_i(\phi)$'s are ϕ-dependent kinematical factors. Therefore, for a given experimental bin in (Q^2, x_B, t), a two parameter-fit of the ϕ-dependence of the BSA yields a model-independent measurement of the real and imaginary parts of the Compton form factor.

These measurements will provide new insight on the partonic structure of the nucleus and will allow us to address novel nuclear effects such as the role of transverse degrees of freedom or the spatial distribution of the strong interactions among partons in nuclei. The comparison between the coherent and the incoherent channels will allow us to access different information on the parton distributions in transverse space: coherent scattering will provide a measurement of the impact parameter dependent parton distributions inside the nucleus, while incoherent scattering will isolate specifically partonic configurations of the bound nucleons.

Due to its spin-0 and high density, the ^{4}He nucleus constitutes an ideal target for disentangling those nuclear effects that can be related to the forward unpolarized EMC effect [17]. Studies of nuclei with different spin, such as the deuteron, involve completely new functions with respect to the forward case therefore making these investigations more difficult. Measurements in

the range $0.1 \lesssim x_B \lesssim 0.6$, and for an appropriate t-range are crucial for both establishing the role of partonic configuration sizes in nuclei, and for discerning among the several competing explanations of the EMC effect. One of the interesting observables in the DVCS process on the proton in the helium nucleus is the ratio of beam-spin asymmetries for the bound and free protons $R^p = \frac{A_{LU}^{incoh}}{A_{LU}^{p}}$, where A_{LU}^{incoh} is the beam spin asymmetry on the bound proton in the helium measured in the proposed experiment, and A_{LU}^{p} is beam spin asymmetry on free proton which will be measured with CLAS12 in a separate experiment [18]. This is so-called generalized EMC effect measured at non-zero four-momentum transfer not accessible in inclusive DIS. As shown in Ref. [9], the role of partonic transverse degrees of freedom, both in momentum and coordinate space, is enhanced in the generalized EMC effect (acessable in both coherent and incoherent DVCS on helium), thus predicting an enhancement of signals of nuclear effects with respect to the forward case. Although the increase of this sensitivity with increasing of $|t|$ is confirmed in Ref. [19], the magnitude of the deviation of the asymmetry A_{LU}^{incoh} of the bound proton from the free proton case is different. The proposed experiment would be able to differentiate between various model predictions of the nuclear medium effects.

Recently we conducted an experiment in Hall-B at Jefferson Lab E08-024 [16] to study DVCS on ^{4}He at 6 GeV electron beam energy. This experiment utilized a radial time projection chamber for the detection of the recoil α-particle to identify the exclusive reaction channel. The newly built detector performed well and the data from this CLAS experiment is currently being calibrated. A similar experiment using 11 GeV polarized electron beam of the upgraded JLab electron accelerator would be a natural extension of this experiment which would allow to access higher values of Q^2 and a larger range in x_B.

In this letter we propose to measure coherent DVCS beam spin asymmetries in order to extract in a model independent way both the real and imaginary parts of the ^{4}He nuclear Compton form factors $\mathcal{H}_A(x_B, t)$. The coherent channel $e\ ^4He \to e'\gamma\ ^4He$, will be identified by measuring all outgoing particles.

We will also simultaneously measure the incoherent DVCS BSA on bound proton and neutron to investigate the modification of the nucleon structure inside of helium nucleus. For the case of the proton, $e\ ^4He \to e'\gamma p\ ^3H$, we can detect all particles in the final state including the recoil tritium in the backward kinematics in order to suppress the final state interaction and to ensure that the scattering occurred on the proton. In the case of incoherent DVCS on bound neutron, $e\ ^4He \to e'\gamma n\ ^3He$, we will detect all particles in the final state except neutron. The exclusivity will be checked using the missing mass technique. Measurements of the momentum of the ^3He and ^3H will allow us to measure the asymmetry as a function of the recoil momentum and the

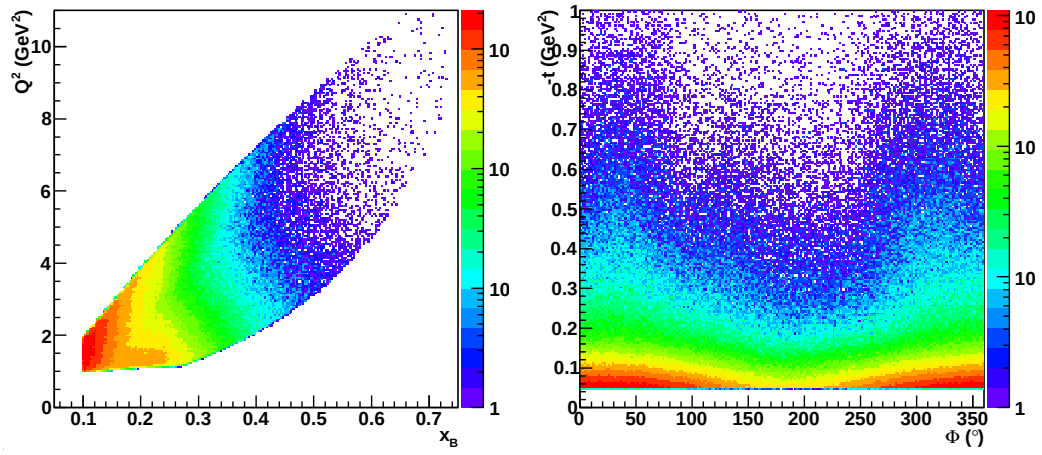

Fig. 3. Kinematic coverage of CLAS12 from a fast Monte-Carlo simulations for coherent DVCS with 11 GeV electron beam incident on the helium target. Q^2 versus x_B is on the left panel, $-t$ versus ϕ is shown on the right panel.

Bjorken variable x_B. The generalized EMC ratio R^p for proton can be calculated as the ratio of the BSA on bound proton measured in this experiment to the asymmetry from the experiments on proton target. As for the generalized EMC ratio for neutron, we will determine the R^n ratio completely from this experiment by interpreting the asymmetry at the lowest recoil momenta determined from the same data as the asymmetry on a free neutron.

The BSA will be experimentally determined as the following ratio:

$$A_{LU} = \frac{1}{P_B} \frac{N^+ - N^-}{N^+ + N^-}, \tag{3}$$

where P_B is the beam polarization, and N^+ and N^- are the number of events detected with positive and negative helicity of electrons, respectively. The proposed experimental setup for the DVCS experiment at 11 GeV includes the basic CLAS12 detector to detect the scattered electron and the outgoing proton (for incoherent channel), and a new dedicated detector to detect the recoil nuclei and to identify the exclusive coherent DVCS process on helium. Detection of all three particles in the final state will allow us to suppress the background from π^0 electroproduction. The remaining contribution from pion background into the beam-spin asymmetry can be subtracted by measuring simultaneously the BSA of the π^0 electroproduction process. This technique has been successfully used in the analysis of DVCS data from proton [14].

For the proposed setup, the kinematic coverage for coherent process as expected from our parametrized Fast Monte-Carlo (FastMC) [20] simulations is illustrated in Fig. 3. The Q^2 range in this experiment will be extended up to 8 GeV^2, while the lowest four-momentum transfer $-t$ will be ~ 0.1 GeV^2.

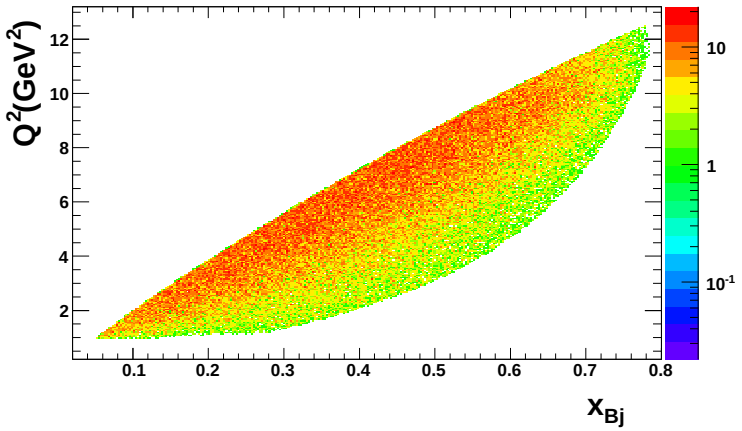

Fig. 4. Expected kinematic coverage of CLAS12, IC and a recoil detector for coherent DVCS on deuteron for Q^2 and x_B

Note that the access to large Q^2 values while keeping $\frac{-t}{Q^2} \ll 1$ is essential for the factorization of the soft and hard scattering part of the DVCS amplitude.

2.2 Coherent DVCS on deuterium target

Deep inelastic scattering processes in the deuteron have been used mainly as the source of information on unpolarized and polarized distributions of a neutron in the forward limit. With the advent of DVCS it became possible to study GPDs of a deuteron as a whole leaving it intact in the final state. Due to the fact that it is a spin-1 object there are entirely new functions appearing which could give us a deeper understanding of this nucleus in terms of its fundamental degrees of freedom. The nine GPDs for a spin-1 object have been given in Ref. [21] and their properties have been discussed in detail in Ref. [22]. Sum rules relate these GPD's to the usual deuteron form factors G_i(i=1,3), which are linear combinations of charge monopole G_C, magnetic dipole G_M, and charge quadrupole, G_Q. The unique feature of these relations is the fact that $G_3(t)$ form factor is totally dominated by the charge quadrupole $G_Q(t)$ [23] and allows us to access the H_3 GPD via beam-spin asymmetry measurements. This will be the first measurement of the partonic structure function of the deuteron related in the forward limit to charge quadrupole, and not only to charge and magnetic form factors, which can not be decomposed into simple additive sum of the proton and neutron. Using the results of these measurements we can access the partonic structure of the deuteron treated as a single hadron, which is irreducible to the partonic structure of its nucleon constituents.

We propose to measure the beam-spin asymmetries in the coherent DVCS

scattering process on deuteron target using CLAS12 detector. The scattered electron will be detected in CLAS12 while the recoil deuteron will be measured in the newly developed detector package installed close to the interaction region. The real photon from the DVCS process will be measured in the inner and forward electromagnetic calorimeters of CLAS12. The kinematical coverage of the experimental setup consisting of CLAS12, the inner calorimeter and a recoil detector is shown in Fig. 4. It illustrates the expected acceptance in Q^2 and x_B variables. These events were uniformly generated in the reaction's phase space, and the detector acceptance was determined using the FastMC package [20].

2.3 Neutron DVCS using deuterium and helium targets

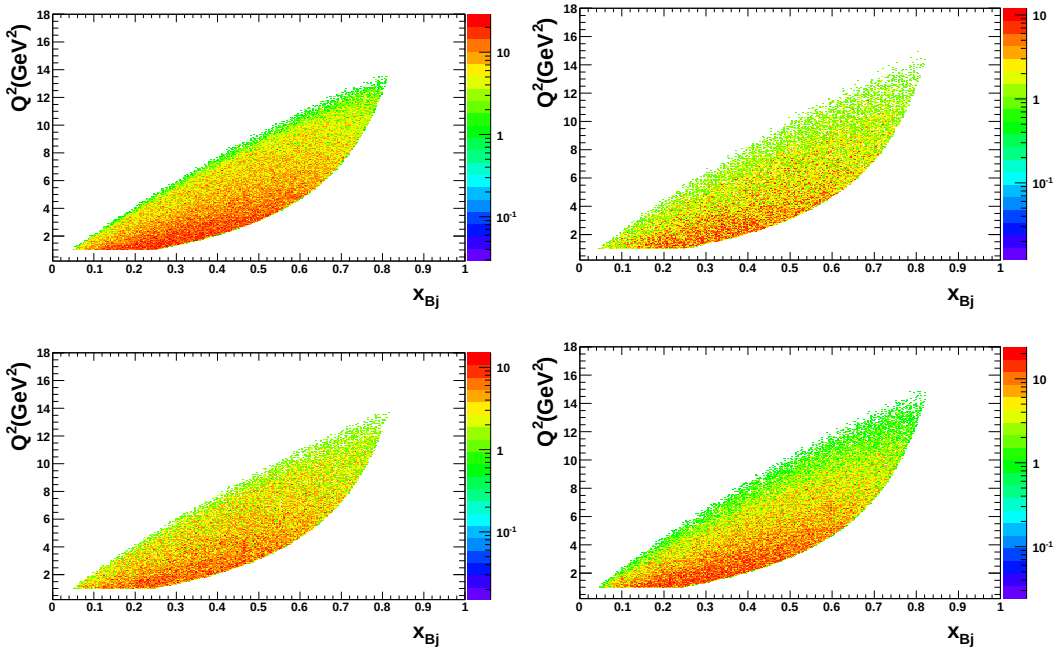

Fig. 5. Q^2 as a function of x_B, for incoherent neutron DVCS events. Top panel left (right): scattering off deuterium target with recoil proton momentum between 20 and 100 MeV (above 100 MeV). Bottom panel left (right): scattering off ^{4}He target with recoil ^{3}He spectator momentum between 50 and 200 MeV (above 200 MeV)

The neutron and proton DVCS are complementary to each other. While the latter gives constraints on GPD H and $\widetilde{H}$, the former gives access to the GPD E leading to the determination of the total angular momentum carried by the quarks in the nucleon (the Ji sum rule [24]):

$$J_q = \frac{1}{2}\int_{-1}^{+1} dx\, x\, [H^q(x,\xi,t=0) + E^q(x,\xi,t=0)] \qquad (4)$$

Furthermore, measurement of the same GPD for proton and neutron will allow for its flavor decomposition.

In this letter, we propose to measure DVCS beam spin asymmetry for quasi-free neutron using an 11 GeV polarized electron beam off deuterium target by tagging the low momentum recoil spectator proton. For neutron DVCS, it was shown [25] that the dominating contribution to the asymmetry amplitude is mostly coming from the GPD E, the least known of the GPDs.

A Monte-Carlo event generator was developed [26] to study the kinematics of the incoherent neutron/proton DVCS reaction from ^{2}H and ^{4}He targets. The DVCS amplitude is calculated following the BMK formalism [27]. We also intend to measure bound neutron (proton) DVCS beam spin asymmetry off ^4He target by detecting the recoil spectator ^{3}He (^{3}H). Fig. 5 shows the distribution of neutron DVCS events accepted in CLAS12 in the $x_B - Q^2$ plane. The following cuts were applied: $W^2 > 4$ GeV^2, $Q^2 > 1$ GeV^2 and $-t > 0.1$ GeV^2.

2.4 Exclusive π^0 electroproduction on helium

Exclusive pion electroproduction on proton in deep inelastic regime has been a subject of extensive studies during the last decade. Factorization into a hard partonic subprocess and into a soft part described by GPDs and wave functions of the mesons was explained in Ref [28]. Goloskokov and Kroll [29] pointed out that the description of pion electroproduction on proton in terms of the corresponding chirally-even GPDs underestimates the experimental data, and that there should be a significant contribution from the transversely polarized photons. Therefore, they concluded that one may need to consider effects from the helicity-flip proton GPDs related to the transverse momentum dependent parton distributions [30].

Following that example, in this letter we would like to consider exclusive pion electroproduction on helium target. Although in the lowest order the coherent DVCS process off ^{4}He is sensitive to a single chirally-even GPD, the spin-0 target in general is described by two twist-2 GPDs [31]. One of these GPDs, H^A is chirally-even, while the other one, H_T^A is chirally-odd. By measuring the single beam spin asymmetry from the DVCS process we can access the $\mathcal{H}^{\mathcal{A}}$ Compton form factor. In order to determine the Compton form factor corresponding to chirally-odd H_T^A we need at least another experimental observable in addition to the beam spin asymmetry from DVCS. One of the possible choices is the beam spin asymmetry from the single π^0 electroproduction on helium.

For scalar targets such as ^{4}He two helicity amplitude combinations contribute [32]. By denoting the helicity amplitudes as $f_{\Lambda_\gamma \Lambda, 0\Lambda'}$ where Λ_γ is the photon

helicity and Λ (Λ') the helicity of the incoming (outgoing) hadronic system, one has that the following two amplitudes appear, $f_{10,00}$ and $f_{00,00}$. The $f_{10,00}$ amplitude corresponds to transverse photons, while $f_{00,00}$ amplitude is due to longitudinal photons. For the helicity amplitudes one can write:

$$f_{\Lambda_{\gamma^*},0;0,0} = \sum_{\lambda,\lambda'} g_{\Lambda_{\gamma^*},\lambda;0,\lambda'} C_{0,\lambda';0,\lambda}. \tag{5}$$

where $C_{0,\lambda';0,\lambda}$ are the "quark-nucleus" helicity amplitudes that depend on x_{Bj}, t and Q^2 while implicitly containing an integration over unobserved quark and nucleon momenta. The $g_{\Lambda_{\gamma^*},\lambda;0,\lambda'}$ are helicity amplitudes for the elementary processes described by perturbative QCD. By considering the nucleus as a composite target the helicity amplitudes can be written in terms of the quark-nucleon helicity amplitudes, $A_{\Lambda'_N\lambda';\Lambda_N,\lambda'}$, and of the nucleon-nucleus ones, $B_{0,\Lambda'_N;0,\Lambda_N}$

$$C_{0,\lambda';0,\lambda} = \sum_{\Lambda_N,\Lambda'_N} \int d^4\, P\, B_{0,\Lambda'_N;0,\Lambda_N} A_{\Lambda'_N\lambda';\Lambda_N,\lambda'} \tag{6}$$

Whether $C_{0,\lambda';0,\lambda}$ can be interpreted as a chiral even or a chiral odd quantity, proportional to either H^A, or H_T^A depends on the coupling of the π^0 being axial vector ($\gamma_\mu\gamma_5$) or pseudo-scalar (γ_5) [33]. The axial vector coupling can be present only for longitudinally polarized photons ($\Lambda_\gamma = 0 \Rightarrow f_{00,00}$). Therefore, the presence of a non-zero transverse structure function would confirm a sizable contribution of transversity in this channel [33]. For instance, without a contribution of H_T^A in the exclusive π^0 channel the beam spin asymmetry should be negligible. By measuring the BSA for this channel we can actually access the Compton form factor corresponding to H_T^A by analyzing the DVCS and π^0 channels. Note that another way of isolating the H_T^A is to measure the exclusive π^0 electroproduction cross section and to perform a Rosenbluth separation because the σ_T structure function is sensitive only to the H_T^A GPD.

We propose to measure the beam spin asymmetry of exclusive π^0 electroproduction, which can be done in parallel to DVCS measurements described in Sec. 2.1. The scattered electron will be detected in CLAS12, while the neutral pions can be reconstructed from the two photons detected in the inner or the forward electromagnetic calorimeters. The coherent channel will be identified by detecting the intact ^{4}He nucleus in the low momentum recoil detector.

2.5 The Pion Structure Function from the H(e,e'p)X Reaction

The meson cloud of a nucleon contributes to electron-proton Deep Inelastic Scattering (DIS), as pointed out by Sullivan [34]. This so called Sullivan process implies that the nucleon parton distributions contain a component that

can be attributed to the meson cloud. One of the consequences of the Sullivan process is the prediction of a quark flavor asymmetry in the nucleon sea [35]. Such a flavor asymmetry of the quark sea was first measured by the NMC experiment [36] and later independently confirmed by Drell-Yan experiments [37–39]. Understanding the origins of this asymmetry has attracted considerable theoretical effort and one of the models which successfully describes the x-dependence of the sea quark flavor asymmetry, is the meson cloud model. The success of the meson cloud model implies that a direct measurement of the meson cloud via DIS should be feasible. The idea is that the meson cloud in the nucleon can be considered as a virtual target to be probed by various hard processes such as DIS.

Recently, the meson structure function was measured at the HERA e-p collider where forward going neutrons and protons were tagged in coincidence with the DIS events [40]. However, the results from HERA are limited to very low x, where no other independent measurement of the pion structure function exists. At JLab energies one can probe the high x region, where together with the pionic Drell-Yan experiments one can provide independent stringent tests of the meson cloud model. Moreover, the large angular and kinematic coverage of the recoiling proton or proton pair in CLAS12 will allow detailed study of the Sullivan process as a function recoil momentum and angles.

We propose to measure the semi-inclusive reaction p(e,e'p)X to study the π^0 cloud of the proton and D(e,e'pp$_S$)X to study the π^- cloud of the neutron, for Q^2 >1 (GeV/c)^2 at very low proton momentum (200 - 400 MeV/c). The kinematics for the measurement will be chosen so that the deep inelastic scattering occurs from the pion cloud surrounding the proton (neutron). The low momentum protons ensure that the virtual pions have a small three momentum and consequently, the pion cloud is spatially large. Thus the key to this experimental technique is to measure the low-energy recoil proton in coincidence with the scattered electron, which can be achieved by employing the CLAS12 to detect the scattered electrons and a recoil detector to detect the scattered protons.

In this experiment we will measure the semi-inclusive structure function of the leading proton, $F_2^{LP(4)}$, which is related to the measured cross-section as;

$$\frac{d^4\sigma(ep \rightarrow e^{'}Xp^{'})}{dxdQ^2dydt} = \frac{4\pi\alpha^2}{xQ^4}\left(1 - y + \frac{y^2}{2[1+R]}\right)F_2^{LP(4)}(x, Q^2, y, t), \qquad (7)$$

where $y = P.q/P.l$, $Q^2 = -(l - l')^2$, $x = Q^2/(2P.q)$ and $t = (P - P')$ where $P(P')$ are the initial(scattered) proton 4 vector, $q = l - l'$ and $l(l')$ are the initial (scattered) lepton and R is the ratio of the cross-section for longitudinally and transversely polarized virtual photons. The structure function of the leading proton, $F_2^{LP(4)}$ is insensitive to the value of R so we use R=0. The measured cross-section can be integrated over the proton momentum (which is effectively

an integration over t) [40] to obtain the leading proton structure function $F_2^{LP(3)}$. The pion structure function F_2^π can then be extracted from $F_2^{LP(3)}$ using models, such as the Regge model of baryon production. In the Regge model the contribution of a specific exchange i is defined by the product of its flux $f_i(y,t)$ and its structure function F_2^i evaluated at (x_i, Q^2). Thus,

$$F_2^{LP(3)} = \sum_i \left[\int_{t_0}^{t_{min}} f_i(z,t) dt \right] F_2^i(x_i, Q^2), \tag{8}$$

where i is pion, ρ-meson, etc, and the variable t corresponds to the range of p_T analyzed.

The Monte Carlo event generator RAPGAP [41] was used to simulate the phase space of the Sullivan process. RAPGAP describes inclusive and diffractive DIS and has been validated with HERA data and was used to extract pion structure function from the HERA data. The results of the RAPGAP simulation at 11 GeV are shown in Fig. 6. Here $x_L = \frac{p_{N'} \cdot q}{p_N \cdot q} = 1 - \frac{x}{x_\pi}$, W_X is the invariant mass of the target fragment other than the recoil proton, p_N is the momentum of the recoil proton. Only events with invariant mass $W_X > 1$ are used in order to avoid events involving exchange of meson resonances. The $W_X > 1$ cut restricts the lowest recoil proton momentum to $P_p > 0.2$ GeV/c and the lowest momentum transfer square to $|t| > 0.1$ GeV^2. In order to access lower t one can reduce the W_X cut and correct for the contributions from other resonances.

The extraction of the pion structure function will have to be corrected for a number of complications to this simple picture, such as the absorptive effect of other mesons and the non pion-pole contributions. These corrections can be minimized by measuring at the lowest proton momentum and lowest $-t$ possible from the reaction. This minimizes the absorptive correction since at lower momenta the pion cloud is further from the bare nucleon. In addition, the low proton momentum ensures that the higher meson mass exchanges are suppressed by the energy denominator. However, the p(e,e'p)X reaction at 11 GeV is dominated by the diffractive process at low proton momentum, which must be taken into account. These and other corrections will have to be carefully studied when developing a full proposal.

The largest uncertainty in extracting the pion structure function arises from the uncertainty of the pion flux in the framework of the pion cloud model. One of the issues is whether to use the πNN form factors (which are know to better than 5%) or the Reggeized form factor. The difference between these two methods can be as large as 20%. However, by comparing to pionic Drell-Yan data at moderate x (at x=0.5 the pion structure function from pionic Drell-Yan is know to about 5%), we expect to have a measure of the pion flux factor.

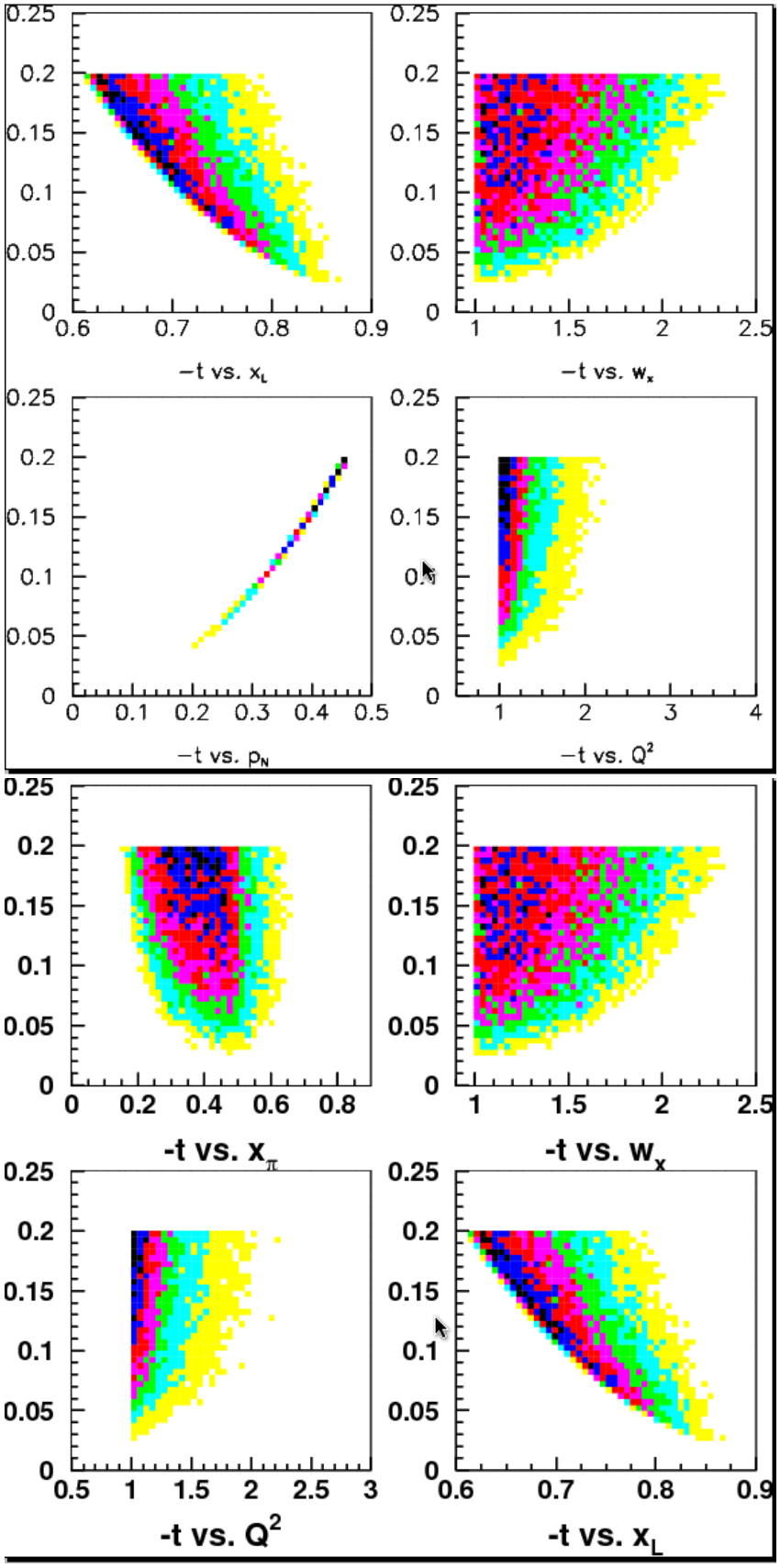

Fig. 6. Phase space simulation of the Sullivan process using the Monte Carlo simulation RAPGAP [41].

For the full proposal we expect to perform more extensive simulations and have a complete estimate of all the corrections and uncertainties in extracting the pion structure function from these semi-inclusive reactions.

2.6 EMC effect and off-shell nucleon structure

The discovery more than twenty years ago, by the EMC Collaboration [17], that the DIS structure functions are modified by the nuclear environment brought quarks and gluons into nuclear physics. A great length of time has passed, but despite concerted efforts on the subject, there is no universally accepted explanation. Many models have been successful in reproducing data for deep inelastic scattering on nuclear targets, but few have described both the DIS and nuclear Drell-Yan experiments. The measurement of the nuclear quark distributions in inclusive DIS processes have not been able to provide enough constraints to distinguish between theoretical models. In order to make progress it is imperative that we move beyond the inclusive experiments.

Melnitchouk et al. [42] suggested that the detection of the recoil nucleus in addition to the scattered electron when scattering off nuclear targets may provide unique information on several long-standing problems, such as the origin of the EMC effect, the possible medium modifications of the nucleon structure functions, and the nature of Nucleon-Nucleon correlations. The semi-inclusive process offers the possibility to investigate the structure function of both weakly and deeply bound nucleons. Measurements of tagged structure functions have been carried in CLAS by the e6 run group to study the EMC effect in deuteron [43] and later by the BoNuS collaboration [44] to extract the F_2^n structure function by tagging the low momentum recoil proton, which is a reliable indicator for scattering off a weakly bound neutron in deuteron. The main goal of the BoNuS measurements is to extract the ratio F_2^n/F_2^p at high x and therefore access the ratio of down to up quark distribution (d/u). By using ^{4}He target and tagging the recoiling ^{3}He and ^{3}H nuclei, one can select scattering off a weakly or deeply bound neutron and proton respectively depending on their off-shellness in the ^{4}He nucleus which can be monitored by the variables $(P_{^3He} - P_{^4He})^2$ and $(P_{^3H} - P_{^4He})^2$. One would measure the F_2 structure functions of a weakly bound neutron in ^{4}He and compare it to the ^{2}H data to detect any nuclear dependence. Since bound neutrons are always off-shell, even when $P_{^3He} = 0$, an extrapolation procedure is needed to extract the free (i.e., on-shell) neutron structure function from the tagged recoil data [45]. This procedure is necessary for neutrons due to the absence of a free neutron target. However it can be quantitatively benchmarked using the ^{3}He tagged data for scattering off a weakly bound proton, and comparing the results to the well measured free proton structure functions. The size of the residual nuclear dependence can be determined using ^{3}He with a tagged deuterium,

and with heavier targets such as ^{12}C with a tagged ^{11}B.

By measuring $F_2^{p,n}$ as a function of x in different bins in the $A-1$ spectator momentum, one can study in detail the dependence of the struture functions on the nucleon off-shellness [46]. This is one of the presumed sources of the EMC effect but is little known theoretically, and is a large source of uncertainty for the determination of the d/u ratio at large x in global PDF fits [47]. The same could be done for bound neutron by comparing it to the quasi-free one from deuterium target.

In addition, the ratio $(F_2^n/F_2^p)^{bound} / (F_2^n/F_2^p)^{free}$ can be measured to extract the distributions of d/u in a free nucleon and compare it to the same ratio for bound nucleon for different spectator momenta. This study will be done with different light nuclei (^{2}H, ^{3}H, ^{3}He or ^{4}He) to study the A dependence. For these measurements, one should pay a close attention to the final state interaction (FSI). In recent papers [42,48], it was suggested that the selection of specific recoils kinematics, especially backward angles, the FSI could be minimized. The high luminosity expected in CLAS12 and high rates capabilities of the recoil detector are important parameters for the success of such measurements since they have to be performed as a function of both the spectator momentum and its angle. This would allow the study of contributions from the target and the current fragmentation regions in addition to the effect of final state interactions. The x coverage for different recoil momenta and for forward and backward detection is shown in Fig. 7. The forward detection is for the spectator fragment whose angle relative to the direction of the virtual photon is below 50 degrees. While the backward detection is for angles above 130 degrees.

The simulation uses a simple model for ^4He nucleus. The constituents are independent nucleons with a Fermi momentum randomized according to a parameterization from reference [49]. The events are generated by Pythia 6 generator with 11 GeV beam on the moving nucleon. A recoil nucleus is added to compensate the initial momentum of the struck nucleon. For the acceptance we use the CLAS12 FastMC [20] except for the recoils. In that case we apply cuts according to the geometry and the energy loss of to the newly built radial time projection chamber for both experiments E-07-009 [50] and E-08-024 [51].

Although the final state interaction is an important effect that can lead to dramatic modification of the spectator kinematics. Ciofi degli Atti et al. [48] model calculations found that the effect of FSI is maximal at 90 degrees, while it is less pronounced at forward direction and is even smaller at backward angles. Experimental tests of the model is crucial to the success of the recoil tagging technique. Therefore our ability to detect the recoil spectator in all directions is very important to all these measurements.

Final state interaction is also expected to play a role in hadronization. It was shown [48] that the transverse region is sensitive to hadronization models. For heavier targets, the global analysis of low energy protons is also a new and complementary way to look at the energy loss during the hadronization process [52]. It suggests looking at the absorbing hadrons instead of measuring the absorbed ones.

In addition to tagging the recoil, one can also detect the product of fragmentation: $e\ ^4He \rightarrow e'\ ^3He\ (^3H)\ \pi^{\pm}$ to study the fragmentation of a bound quark to a hadron where the produced meson is detected in CLAS12 with a high fraction of the virtual photon energy. These measurements would provide us with more insights into the modification of the quark fragmentation in the nuclear medium relative to the vacuum.

For heavy nuclei, there are several semi-inclusive experiments that have been suggested to study the origins of the EMC effect. We consider two types of semi-inclusive processes here. 1.) The ^{12}C(e,e'(A-1))X process where the DIS occurs in a low momentum nucleon and the nucleus (A-1) recoils with low momentum and low excitation energy and is detected in coincidence with the scattered electron. 2.) The process A(e,e'N_2(A-2))X, where DIS occurs on a high momentum nucleon N_1 of a correlated pair, and the nucleon N_2 and nucleus (A-2) recoil with high and low momenta respectively, and are detected in coincidence with the scattered electron.

Ciofi degli Atti *et al.* [53] have shown that the semi-inclusive EMC ratio $R_0(x_{Bj}, Q^2) = \frac{\int_a^b \sigma^{^{12}C} d\vec{P}_{A-1}}{\int_a^b \sigma^{^2H} d\vec{P}_{A-1}}$ integrated over a small momentum interval of the recoil nucleus $\vec{P}_{A-1}$ with $\vec{P}_{A-1} = -\vec{p}_1$, differs dramatically for recoil nuclei that are emitted backward versus forward (see Fig. 8 top panel). Additionally the semi-inclusive ratio is extremely sensitive to the separate contributions to the EMC effect from the s and p shells of the nucleus as shown in Fig. 8(bottom panel), for the backward going recoil nucleus. Only the backward ratios are shown in Fig. 8(bottom panel) because it is less affected by FSI between the (A-1) nucleus and the hadrons resulting from quark hadronization. Note that not only are the different shell contributions well separated but the semi-inclusive EMC effect is much larger than the usual inclusive EMC effect.

These authors have also shown that the ratio $R_2 = \frac{\sigma^{^{12}C}(x_{Bj}, Q^2, \vec{P}_{A-2}, \vec{p}_2)}{\sigma^{^2H}(x_{Bj}, Q^2, \vec{P}_{A-1})}$ can be used to investigate the structure function of deeply bounds nucleons (i.e binding energy dependence of the nucleon structure functions) and can distinguish between different models of the EMC effect such as the binding (x-rescaling) vs the Q^2 rescaling models, as shown in Fig.9.

In addition to studying the origins of the EMC effect, if the nuclei (A-1) and

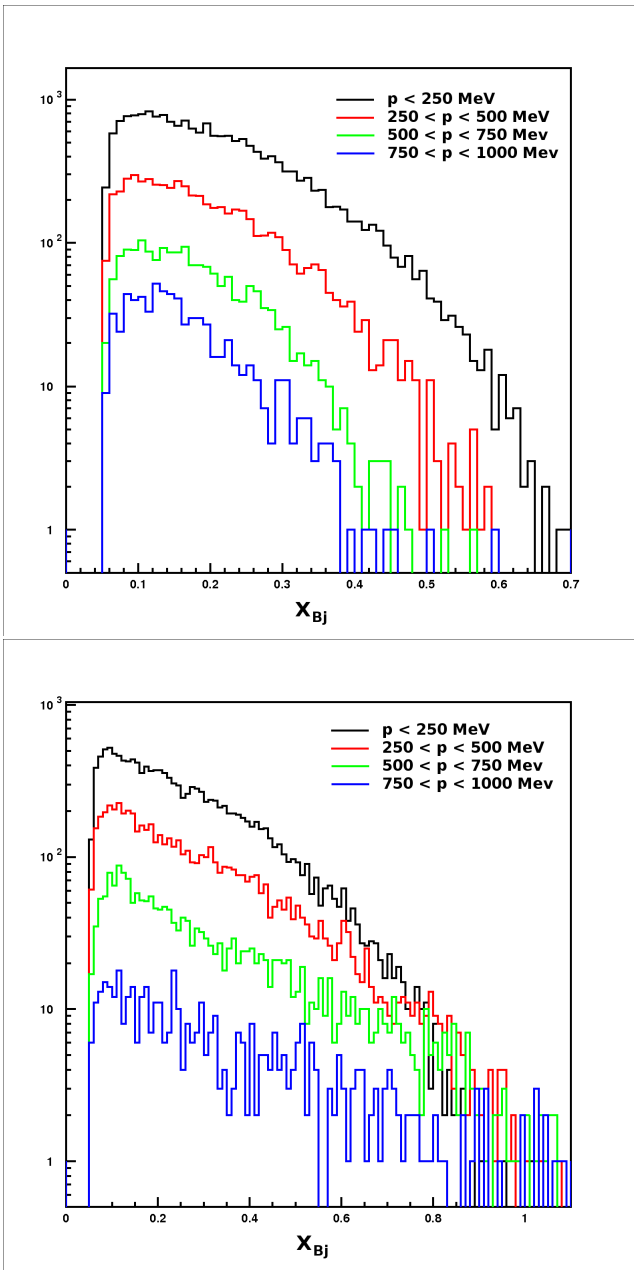

Fig. 7. (Top) x distribution for different recoil spectator momenta when the spectator is detected backward. (Bottom) x distribution for different recoil spectator momenta when the spectator is detected forward (see. text).

(A-2) are detected in coincidence with the scattered electron, this is a clear signal of the absence of FSI; at the same time the cross-section will depend on FSI, therefore the study of its absolute value and A dependence will allow the investigation of the nature of FSI, e.g. hadronization length of the hit quark.

We propose to measure the ratios listed here using solid Carbon dioxide or Oxygen gas targets. The recoil detector along with CLAS12 will allow an investigation of the origins of the EMC effect over a wide range of kinematics

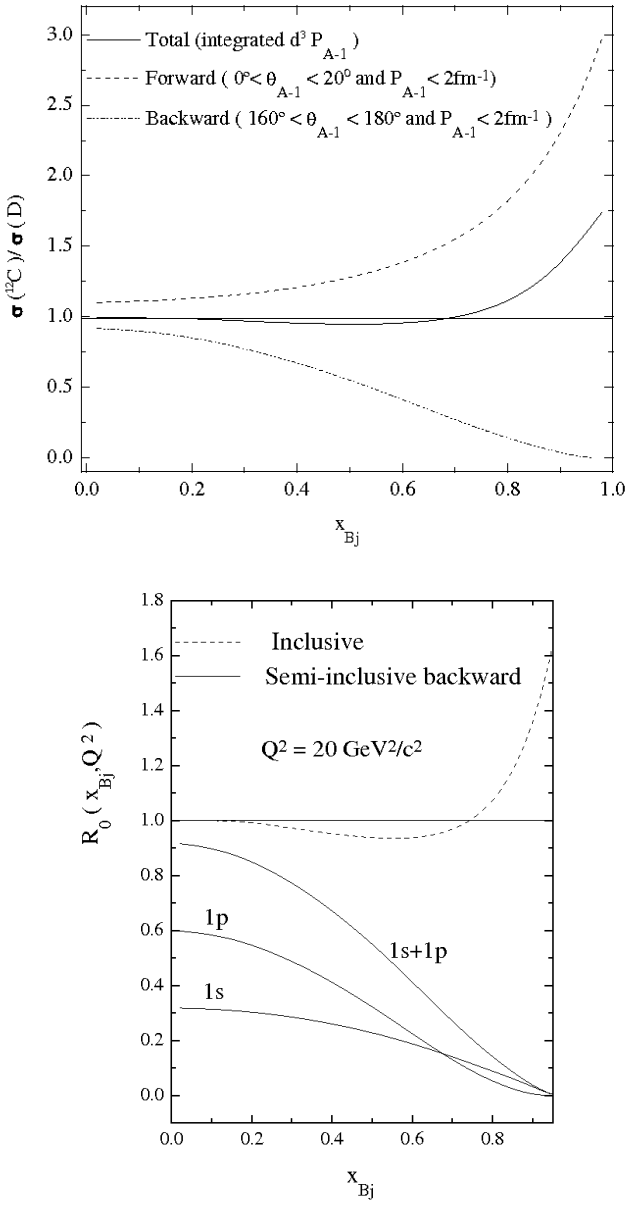

Fig. 8. (Top) The semi-inclusive EMC ratio $\sigma(^{12}C)/\sigma(D) = R_0(x_{Bj}, Q^2)$, corresponding to nuclei emitted backward and forward in the kinematic range shown in the Figure. The full curve is the usual inclusive EMC ratio.(Bottom) The backward semi-inclusive EMC effect on ^{12}C. The dashed curve represents the usual inclusive EMC ratio.

and may help pin down its exact origins.

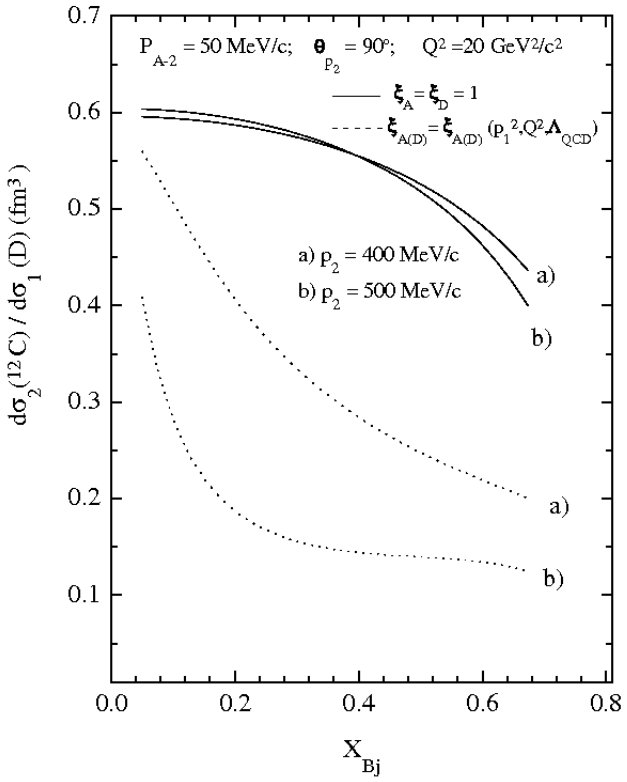

Fig. 9. The ratio R_2 for ^{12}C vs x_{Bj} for fixed value of the momentum of the recoiling (A-2) system P_{A-2} = 50 MeV/c, two different values of the recoiling nucleon N_2, p_2 = 400 MeV/c and 500 MeV/c and fixed emission angle of the nucleon = 90^0. The full lines correspond to the binding model and the dotted line to the Q^2 rescaling model.

2.7 Meson spectroscopy on nuclear target

Another important physics program that will require a low energy recoil detector is the meson spectroscopy in coherent production on light nuclei. Details of these kind of studies are presented in hadron spectroscopy program for CLAS12 submitted as a Letter of Intent to this PAC. Coherent production is used to eliminate physics background arising from associated baryon resonance production. In order to ensure coherent production of a mesonic state, the recoil nuclei must be detected.

Production of mesons in the mass range from 1 to 3 GeV will be studied in all charged modes using neutral and charge exchange reaction on ^{3}H, ^{3}He, and ^{4}He nuclei. Measurements must be carried out at small transferred momentum range, close to t_{min}. Recoil nuclei then will have kinetic energy in the range from 5 MeV to 30 MeV. Decay product of mesons produced in t-channel will be detected in CLAS12, while recoil nuclei will be detected in the low energy

recoil detector. Such an experiment (E-07-009) has already been carried out with CLAS using 6 GeV electron beam, ^{4}He gas target and an RTPC based on cylindrical GEMs [50]. The experiment at 6 GeV searches hybrid mesons in the decay mode of $\pi\eta$ and $\pi\eta'$. At 6 GeV, experimental reach of masses for t-channel mesons is ~ 1.8 GeV. We propose to extend this studies to higher mass range (up 3 GeV) since lattice QCD calculations yield ~ 2 GeV mass for the lightest hybrid meson with exotic quantum numbers $J^{PC} = 1^{-+}$.

3 Experimental Setup

3.1 Baseline CLAS12 instrumentation

The CLAS12 detector is designed to operate with the upgraded Jefferson Lab accelerator at 11 GeV with electron-nucleon luminosity of $L = 1 \times 10^{35} cm^{-2} s^{-1}$. The beam polarization of 85% is already achieved at 6 GeV and is expected to be available after 12 GeV upgrade. The beam polarization in Hall B will be measured by an upgraded Moller polarimeter based on the one currently used at 6 GeV.

The baseline CLAS12 configuration consists of the forward detector and central detector packages. Figure 10 shows the exploded schematic view of the various components of the basic CLAS12 and the inner calorimeter. The proposed experiments do not require modifications to the Forward Detectors (FD) of CLAS12. However the Central Detector (CD) designed for detecting particles with lower momenta at larger angles needs significant modifications to accommodate the experimental requirements. In particular, a low momentum detector will be installed for the detection of recoil hadrons scattered at large angles. The solenoid magnet of the central detector will be used to provide magnetic field for the tracking purposes and for shielding from electrons from Moller scattering.

The High Threshold Cherenkov Counters (HTCC) together with the Forward Calorimeter and the Preshower Calorimeter will provide pion rejection factor of more than 2000 up to momentum of 4.9 GeV, and a rejection factor of 100 above 4.9 GeV.

In the baseline design of CLAS12 the charged particle identification in the forward detector is achieved by utilizing the HTCC, Low Threshold Cherenkov Counters (LTCC) and the Time-of-Flight scintillator arrays (TOF) in conjunction with the tracking information from the Drift Chambers (DC). These detectors systems provide p/π and K/π separation in full momentum range, while in the p/K separation there is a gap between momenta $4-8$ GeV. More-

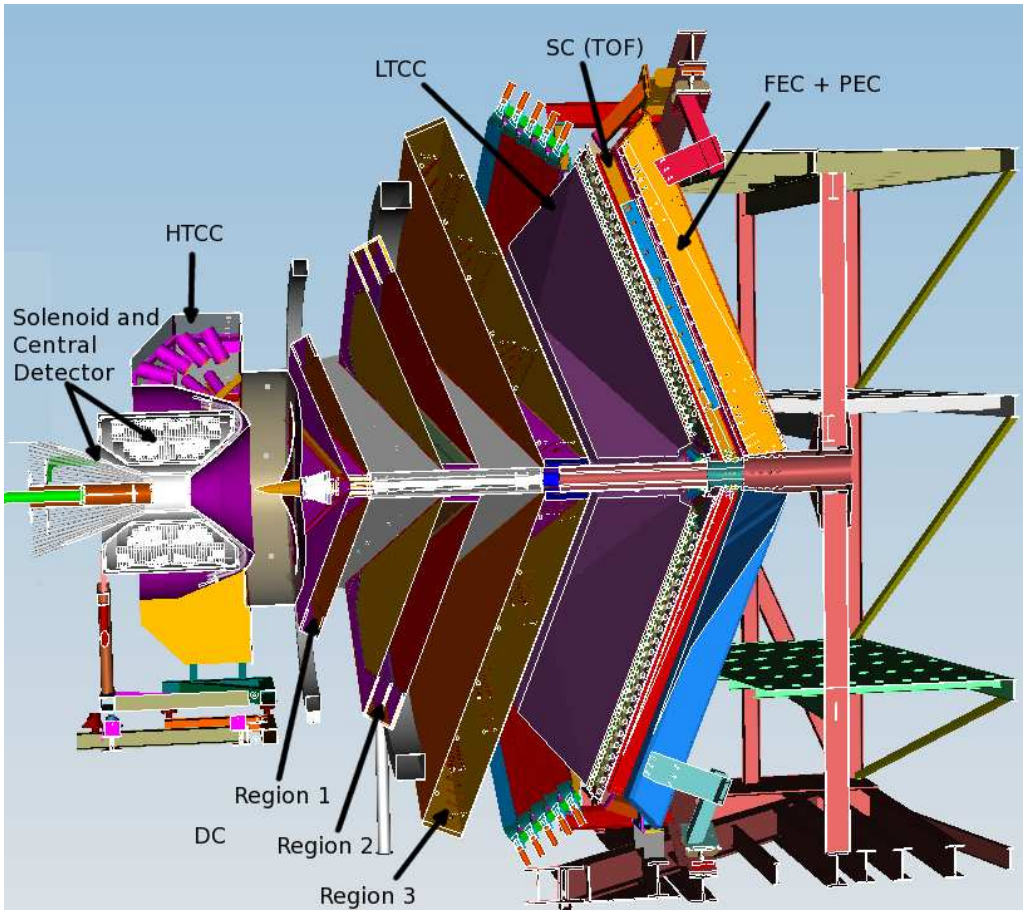

Fig. 10. Schematic drawing of the baseline CLAS12 design showing the main detector components.

over, in the $2.5-5$ GeV momentum region, the π/K separation relies only on the LTCC performance. In general, this PID system is well matched to requirements of the main physics program at 12 GeV. However there are some physics reactions of high interest that cannot be easily accessed without better PID, especially for charged kaon detection. A RICH detector, to be installed in place of the low threshold Cherenkov counter, although not absolutely necessary here, will significantly improve the CLAS12 particle identification overcoming the above limitations.

Some of the experiments described in this letter require photon detection capabilities at small angles. The forward calorimeter with nominal target position covers the angular range from 5° to 40°, while for lower angles a separate photon detector will be needed. This coverage can be achieved by using a calorimeter similar to the Inner Calorimeter (IC) used for the 6 GeV DVCS experiments in Hall B. The IC was built in 2003-2004 and was successfully operated during four different DVCS experiments in CLAS [54],[55],[56] and [51]. It provided an energy resolution of $\frac{\sigma_E}{E} = 4.5\%$ for 1 GeV photons [57].

The parameterization for position resolution for IC

$$\sigma_x = \sigma_y(\text{mm}) \simeq \frac{1.8}{\sqrt{E}} \oplus 0.1 \tag{9}$$

translates into 0.2 mrad for a 9 GeV photon from a point target viewed from a distance of 1.75 meters [58]. A similar photon detector, already suggested in the Jefferson Lab proposal E12-06-119 [18] can provide an angular coverage from 1.5° to 5° for photons with CLAS12.

Additional information on the baseline CLAS12 configuration and the specialized equipment can be found in the document provided as an appendix to all CLAS12 proposals.

3.2 Low energy recoil detector

CLAS12 Central Detector [59], see Fig. 11, is designed to detect and identify charged particles (π-mesons, K-mesons, protons, deuterons ...) in a wide momentum and angular range. However, due to the thickness of layers of the silicon tracker, the minimum momentum for charged particles to be detected in CD is high. For example, for protons the minimum momentum P_{min} is $\sim$ 0.2 GeV, for deuterons P_{min} $\sim$ 0.35 GeV, as can be seen from Fig. 12. Higher mass (A) and charge (Z) particles, e.g. ^3He, ^3H, ^4He, will have even higher detection threshold. This minimum momentum cut-off puts limitations on the kinematical coverage of the experiments which require detection of a low energy recoil particles in coherent scattering reactions on light nuclei or a low energy spectators from scattering of inter-nuclear nucleon.

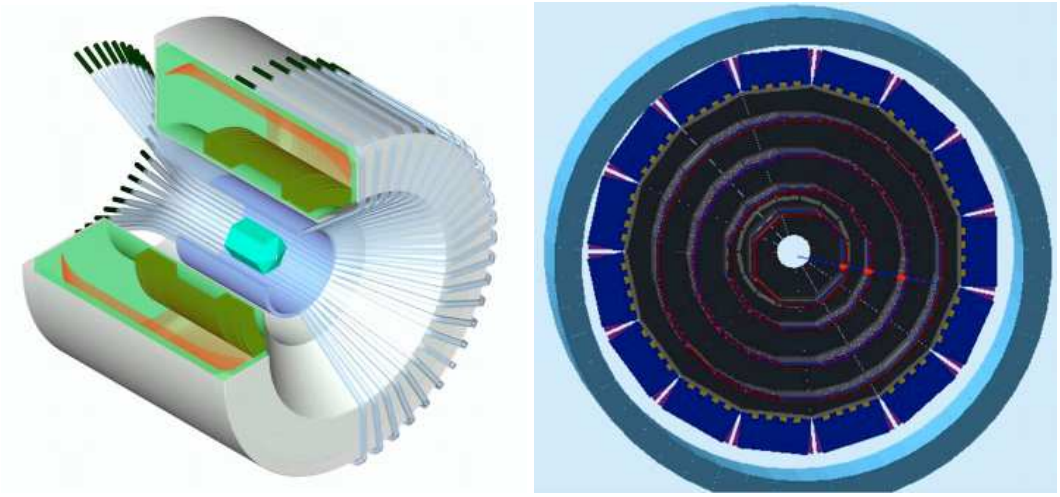

Fig. 11. CLAS12 central detector. Left - 3-D model of the central detector, superconducting solenoid, central time-of-flight counters and silicon vertex tracker. Right - GEANT-4 simulation of 0.2 GeV proton in the central detector [60].

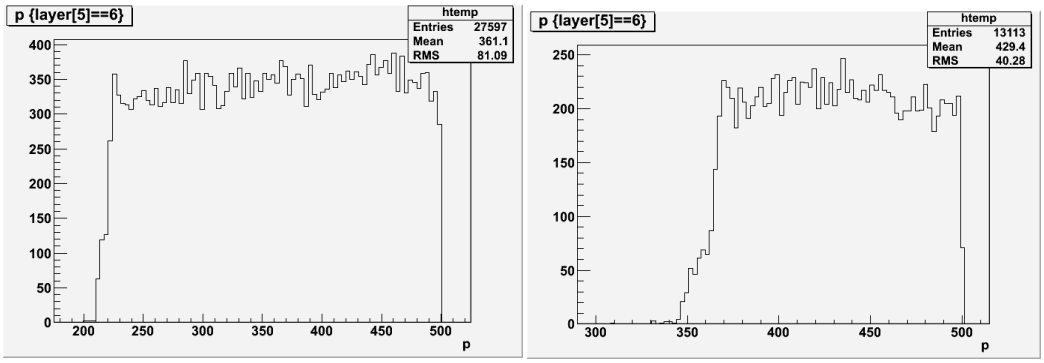

Fig. 12. Momentum distribution of protons (left) and deuterons (right) detected in the CLAS12 CD from GEANT-4 simulations.

For the proposed measurements, we intend to replace silicon tracker in the CLAS12 CD with a detector with much lower detection threshold for charged particles. Low energy recoil detectors with gas targets have already being used in Hall B together with the CLAS detector in electroproduction experiments at 6 GeV. Two CLAS run periods, BoNuS [61] and eg6 [62], successfully used a Radial Time-projection Chamber (RTPC) based on Gas Electron Multipliers (GEM). BoNuS run, experiment E03-012 [44], was the first to build and use the RTPC based on cylindrical GEMs together with deuterium gas target at 7 atmosphere pressure. The purpose of the detector was the tagging of low energy ($P > 60$ MeV/c) spectator protons in deep inelastic scattering of high energy electrons off an almost on-shell neutron. The second run period (eg6) consisting of two experiments E-07-009 [50] and E-08-024 [51], used a ^{4}He gas target at 6 atmosphere and a new RTPC to detect recoiling α-particles in coherent scattering of electrons off helium nucleus. The new RTPC was built using the same general principals but with improved characteristics, see Fig. 13. The most notable improvement to the first detector was much higher data rate. New readout system allowed to run CLAS DAQ in full pipeline mode with a trigger rate of 3 kHz and 80% livetime (compared to 0.5 kHz in the first run). Other improvements included fully cylindrical geometry of the drift region and the GEM assembly, see Fig. 14. Elimination of the support wall between the two sides of the detector improved the geometrical acceptance. In order to lower the detection momentum threshold, eg6 run group used a target cell with thinner walls, 30 μm instead of 50 μm used in BoNuS.

For CLAS12 we plan to design and build a new low energy particle detector. There is a conditionally approved 11 GeV proposal [65] (BoNuS11) that is planning to use similar device. The existing RTPC for CLAS has several disadvantages to be used with CLAS12. First, it retains two side readout

Fig. 13. CLAS eg6 RTPC and target assembly.

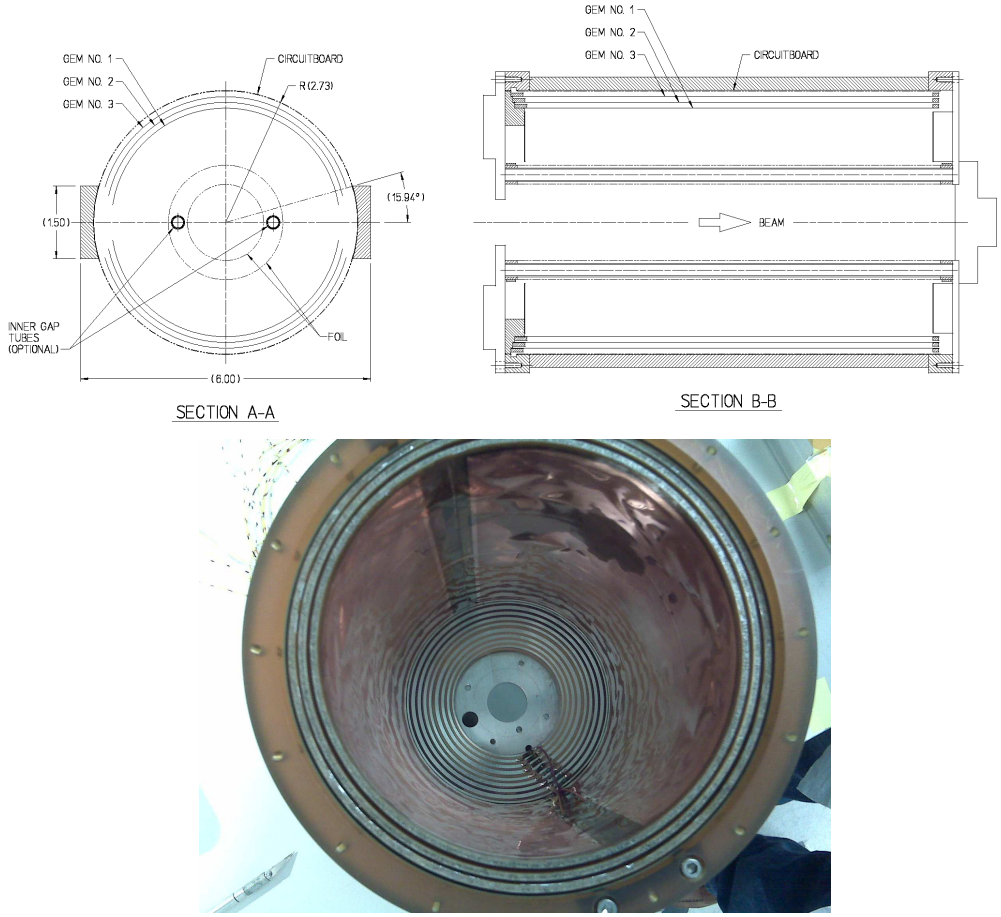

Fig. 14. Design (top) and GEM assembly (bottom) of the eg6 RTPC.

structure, leaving gaps in the GEM coverage of the full azimuthal drift region. The geometry of the detector is defined by the DVCS solenoid magnet that has 24 cm bore. Achieved readout rate is matched with maximum achievable luminosity of CLAS.

The design of a new detector will take full advantage of larger bore of the

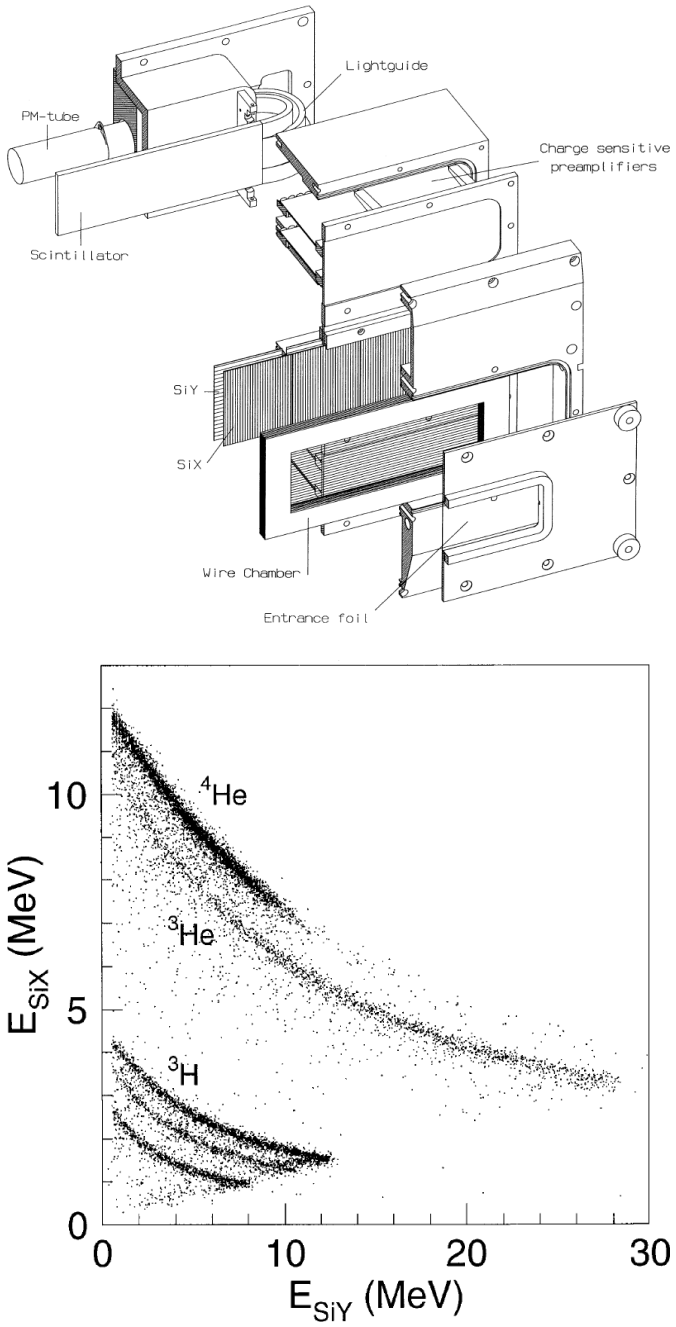

Fig. 15. Top: schematic view of a recoil detector used in AmPS (NIKHEF). Bottom: particle identification using energy loss in silicon strip detectors [63].

CLAS12 five-Tesla solenoid magnet and the high luminosity capability of the CLAS12 detector. With successful run of RTPCs based on the cylindrical GEMs in two experiments, the first choice for a low energy recoil detector for CLAS12 will be a similar detector with better characteristics. With improved technology of GEM manufacturing, it will be straightforward to make a full 2π azimuthal coverage of readout system. Detector volume will be larger to achieve a better energy loss and momentum determination. By the time of

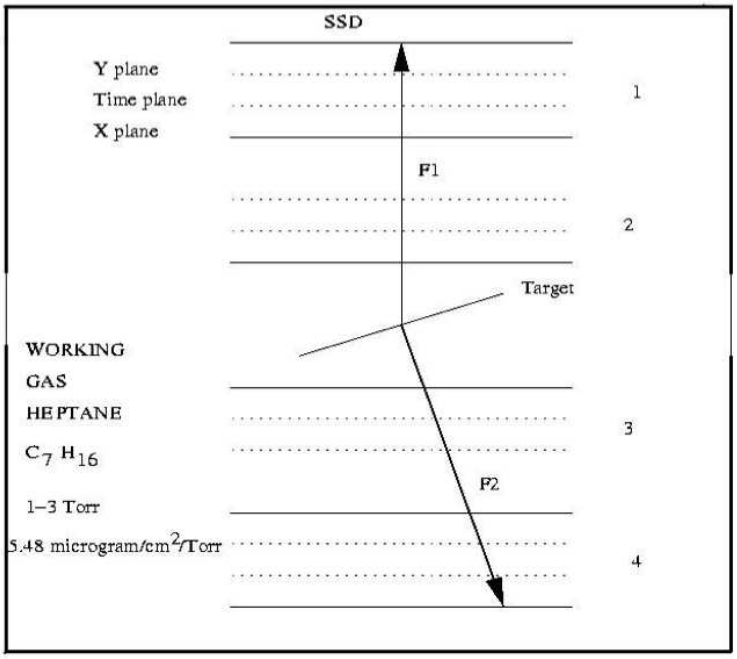

Fig. 16. Schematic sketch of FFD [64].

the development of full proposals we will have options for a new data readout system from RTPC with shorter readout time (current system based on Altro chips has $\sim 100\mu$s readout time for each front end card for 128 channels). The new system must be designed to match the higher DAQ rate capability of CLAS12.

One of the potential issues with the RTPC at high luminosity runs is the rate of accidental tracks that is defined by the drift time of $\sim 5\mu$s. This is more of a problem for inclusive measurements when kinematical constraints cannot be used to filter out accidentals. For this reason, we are looking into a second option for a low energy recoil detector for CLAS12 which will be much faster and will have a good timing measurement to allow for a tight time coincidence with CLAS12. Such detectors have been successfully used before. For example a low pressure recoil detector (LPRD) was used in AmPS (NIKHEF) [63] for internal target experiments, and a fission fragment detector (FFD) was built for the hyper-nuclear experiments in Hall C (JLab) [64] and for the absolute photo-fission studies in MAX-lab (Lund Sweden). In Fig. 15, a schematic view and particle identification in LPRD are shown. The detector consists of two-step avalanche chamber, two layers of silicon strip detectors and a scintillator detector. The kinetic energy detection threshold for different particles in the silicon strip layers of LPRD were as follows: for protons - 3.2 MeV, for deuterons - 4.2 MeV, for ^{3}H - 4.9 MeV, for ^{3}He - 11 MeV, and for ^{4}He - 13 MeV. The detector was operated at 7 mbar gauge pressure.

The schematic of FFD is shown in Fig. 16. The basic concept here is the same. It consists of a multi-wire proportional chamber for position measurements, a timing plane for TOF measurements and solid state detectors mounted just behind the outer chambers for energy loss measurements. The expected timing resolution for these detectors is on the order of ~ 150 ps.

Both of these detectors are fast and they can be used in an high rate environment. In particular these types of detectors can be viable option for electron scattering experiments on solid targets. For the full proposals, all these options for a low energy recoil detector for CLAS12 discussed above will be studied, and the configuration best suited for the physics goals of the experiments will be chosen.

One of the most important components of the low energy particle detection is the target. Both of the CLAS experiments which utilized an RTPC high pressure used gaseous targets. The target gas was confined in a small 6 mm diameter, 30 cm long, cylindrical volume made of kapton (thickness of the target walls was 50 μm for BoNuS target and 30 μm for eg6 target). The gas was separated from beamline vacuum by 15 μm aluminum foils. The target cell wall thickness was the biggest contributor to the minimum momentum limit in the system. Clearly, the smaller the differential pressure between the target gas and the detector gas, the thinner walls can be used (target walls can be eliminated if target and detector are at the same pressure). Lower target pressure, however, will increase the contribution of the beamline windows to the trigger rate. During the BoNuS and eg6 runs the contributions from the entrance and exit windows of the target cell was $\sim 15\% - 25\%$. A possible option for improvement is to use thinner windows, e.g. $\sim 10\mu$m Be windows. This will yield a factor two gain in the thickness, and, therefore, for the same ratio of the target material thickness to the material thickness of the windows one can use twice lower target gas pressure. This in turn will allow us to use target cells with thinner than 30 μm wall thickness. Another option is to design a detector that can operate at a higher pressure. But for any low pressure detector design for CLAS12 it is imperative that the design includes a design for the corresponding target as well.

4 Summary

In summary, we described a broad experimental program to be carried out using the CLAS12 detector, which would strongly benefit from a new low energy recoil detector. The described experiments include measurements of the beam spin asymmetries in DVCS and exclusive π^0 electroproduction channels on helium target, coherent and incoherent DVCS on deuterium, in order to study the Generalized Parton Distributions of nucleon and nuclei, and the

modification of the structure of the nucleon inside nuclei. The measurements of the EMC effect, now widely considered as one of the traditional methods of studying the effects of nuclear medium on nucleons, will be carried out using a novel technique of tagging the recoil fragments. This will increase the sensitivity of the experiments to different ingredients of the theoretical models developed to describe the EMC effect. Another exciting measurement which will benefit from the new recoil detector is the measurement of the pion structure function off hydrogen and deuterium. The meson spectroscopy program using helium target, which currently is carried out at 6 GeV with CLAS, will strongly benefit from accessing the higher mass regions of mesons with 11 GeV electron beam. Again, it is absolutely crucial for this experiments to ensure the coherence of the scattering process by detecting the helium nucleus intact.

Although some of these experiments require different experimental conditions, it is highly desirable that they can be performed using a single recoil detector. Three different designs are considered which could accommodate the requirements of these different measurements. The feasibility of each measurement needs to be confirmed before a proposal is presented for approval. A comprehensive study, which will include the general detector layout, detailed detector simulations and design of readout electronics, will be conducted in the process of preparing the full experimental proposals for the individual experiments described in this letter and the already accepted one (BoNuS11) since there is an important overlap and strong collaboration between the two groups.

References

[1] D. Müller, D. Robaschick, B. Geyer, F.M. Dittes, and J. Hořejši. Fortsch. Phys., 42:101, 1994.

[2] M. Diehl. Generalized parton distributions. Phys. Rept., 388:41–277, 2003.

[3] A. V. Belitsky and A. V. Radyushkin. Unraveling hadron structure with generalized parton distributions. Phys. Rept., 418:1–387, 2005.

[4] Dieter Mueller, D. Robaschik, B. Geyer, F. M. Dittes, and J. Horejsi. Wave functions, evolution equations and evolution kernels from light-ray operators of QCD. Fortschr. Phys., 42:101, 1994.

[5] Matthias Burkardt. Impact parameter dependent parton distributions and off-forward parton distributions for zeta $\to$ 0. Phys. Rev., D62:071503, 2000.

[6] M. Diehl. Generalized parton distributions in impact parameter space. Eur. Phys. J., C25:223–232, 2002.

[7] Andrei V. Belitsky and Dieter Mueller. Nucleon hologram with exclusive leptoproduction. Nucl. Phys., A711:118–126, 2002.

[8] Matthias Burkardt. Transverse deformation of parton distributions and transversity decomposition of angular momentum. Phys. Rev., D72:094020, 2005.

[9] S. Liuti and S. K. Taneja. Microscopic description of deeply virtual Compton scattering off spin-0 nuclei. Phys. Rev., C72:032201, 2005.

[10] V. Guzey and M. Siddikov. On the A-dependence of nuclear generalized parton distributions. J. Phys., G32:251–268, 2006.

[11] M. V. Polyakov. Generalized parton distributions and strong forces inside nucleons and nuclei. Phys. Lett., B555:57–62, 2003.

[12] Alberto Accardi, D. Grunewald, V. Muccifora, and H. J. Pirner. Atomic mass dependence of hadron production in deep inelastic scattering on nuclei. Nucl. Phys., A761:67–91, 2005.

[13] C. Munoz Camacho et al. Scaling tests of the cross section for deeply virtual Compton scattering. Phys. Rev. Lett., 97:262002, 2006.

[14] F. X. Girod et al. Deeply Virtual Compton Scattering Beam-Spin Asymmetries. Phys. Rev. Lett., 100:162002, 2008.

[15] V. Guzey and M. Strikman. DVCS on spinless nuclear targets in impulse approximation. Phys. Rev., C68:015204, 2003.

[16] K. Hafidi, F.-X. Girod, E. Voutier, H. Egiyan, S. Liuti, et al. Deeply Virtual Compton Scattering off ^{4}He. JLab Experiment E08-024, 2008.

[17] J. J. Aubert et al. The ratio of the nucleon structure functions $F2_n$ for iron and deuterium. Phys. Lett., B123:275, 1983.

[18] F. Sabatie, H. Egiyan, L. Elouadrhiri, A. Biselli, et al. Deeply Virtual Compton Scattering with CLAS12 at 11 GeV. JLab Experiment E12-06-119, 2006.

[19] V. Guzey, A. W. Thomas, and K. Tsushima. Medium modifications of the bound nucleon GPDs and incoherent DVCS on nuclear targets. Phys. Lett., B673:9–14, 2009.

[20] M. Mestayer, K. Mikhaylov, H. Avakian, et al. FastMC fast detector simulation program for CLAS12, unpublished, 2006.

[21] Edgar R. Berger, F. Cano, M. Diehl, and B. Pire. Generalized parton distributions in the deuteron. Phys. Rev. Lett., 87:142302, 2001.

[22] A. Kirchner and Dieter Mueller. Deeply virtual Compton scattering off nuclei. Eur. Phys. J., C32:347–375, 2003.

[23] M. Amarian, H. Juengst, F. Sabatie, L. Elouadrhiri, et al. Deeply Virtual Compton Scattering on the Deuteron with CLAS at 6 GeV. JLab Proposal PR-06-015, 2006.

[24] X. Ji. Phys. Rev., D55:7114, 1997.

[25] K. Goeke, M.V. Polyakov, and M. Vanderhaeghen. Prog. Part. Nucl. Phys., 47:401, 2001.

[26] A. El Alaoui and E. Voutier. An event generator for electroproduction of photons incoherently. CLAS Note 2009-024.

[27] A.V. Belitsky, D. Müller, and A. Kirchner. Nucl. Phys., B629:323, 2002.

[28] John C. Collins, Leonid Frankfurt, and Mark Strikman. Factorization for hard exclusive electroproduction of mesons in QCD. Phys. Rev., D56:2982–3006, 1997.

[29] S. V. Goloskokov and P. Kroll. An attempt to understand exclusive pi+ electroproduction. 2009.

[30] S. Meissner, A. Metz, and K. Goeke. Relations between generalized and transverse momentum dependent parton distributions. Phys. Rev., D76:034002, 2007.

[31] Sigfrido Boffi and Barbara Pasquini. Generalized parton distributions and the structure of the nucleon. Riv. Nuovo Cim., 30:387, 2007.

[32] G. Goldstein and S. Liuiti. to be published.

[33] S. Liuti and G. Goldstein. Private Communication, 2009.

[34] J. D. Sullivan. One pion exchange and deep inelastic electron - nucleon scattering. Phys. Rev., D5:1732–1737, 1972.

[35] Anthony William Thomas. A Limit on the Pionic Component of the Nucleon Through SU(3) Flavor Breaking in the Sea. Phys. Lett., B126:97, 1983.

[36] P. Amaudruz et al. The Gottfried sum from the ratio F2(n) / F2(p). Phys. Rev. Lett., 66:2712–2715, 1991.

[37] E. A. Hawker et al. Measurement of the light antiquark flavor asymmetry in the nucleon sea. Phys. Rev. Lett., 80:3715–3718, 1998.

[38] J. C. Peng et al. anti-d/anti-u asymmetry and the origin of the nucleon sea. Phys. Rev., D58:092004, 1998.

[39] R. S. Towell et al. Improved measurement of the anti-d/anti-u asymmetry in the nucleon sea. Phys. Rev., D64:052002, 2001.

[40] C. Adloff et al. Measurement of leading proton and neutron production in deep inelastic scattering at HERA. Eur. Phys. J., C6:587–602, 1999.

[41] H. Jung. Comp. Phys. Comm, 86:147, 1995.

[42] W. Melnitchouk, M. Sargsian, and M. I. Strikman. Probing the origin of the EMC effect via tagged structure functions of the deuteron. Z. Phys., A359:99–109, 1997.

[43] A. V. Klimenko et al. Electron scattering from high-momentum neutrons in deuterium. Phys. Rev., C73:035212, 2006.

[44] http://www.jlab.org/exp_prog/experiments/summaries/E03-012.ps, 2003.

[45] Misak Sargsian and Mark Strikman. Model independent method for determination of the DIS structure of free neutron. Phys. Lett., B639:223–231, 2006.

[46] C. Ciofi degli Atti, L. L. Frankfurt, L. P. Kaptari, and M. I. Strikman. On the dependence of the wave function of a bound nucleon on its momentum and the EMC effect. Phys. Rev., C76:055206, 2007.

[47] A. Accardi et al. New parton distributions from large-x and low-Q^2 data. 2009.

[48] Claudio Ciofi degli Atti, L. P. Kaptari, and B. Z. Kopeliovich. Final state interaction effects in semi-inclusive DIS off the deuteron. Eur. Phys. J., A19:145–151, 2004.

[49] Claudio Ciofi degli Atti and S. Simula. Realistic model of the nucleon spectral function in few and many nucleon systems. Phys. Rev., C53:1689, 1996.

[50] http://www.jlab.org/exp_prog/proposals/07/PR-07-009.pdf, 2007.

[51] http://www.jlab.org/exp_prog/proposals/08/PR-08-024.pdf, 2008.

[52] C. Ciofi degli Atti and B. Z. Kopeliovich. Time evolution of hadronization and grey tracks in DIS off nuclei. Phys. Lett., B606:281–287, 2005.

[53] Claudio Ciofi degli Atti, L. P. Kaptari, and S. Scopetta. Semi-inclusive deep inelastic lepton scattering off complex nuclei. Eur. Phys. J., A5:191–207, 1999.

[54] V. Burkert, L. Elouadrhiri, M. Garçon, and S. Stepanyan. Deeply Virtual Compton Scattering with CLAS at 6 GeV. JLab Experiment E01-113, 2001.

[55] V. Burkert, L. Elouadrhiri, M. Garçon, R. Niyazov, and S. Stepanyan. Deeply Virtual Compton Scattering with CLAS at 6 GeV. JLab Experiment E06-003, 2003.

[56] A. Biselli, L. Elouadrhiri, K. Joo, and S. Niccolai. Deeply Virtual Compton Scattering at 6 GeV with polarized target and polarized beam using the CLAS Detector. JLab Experiment E05-114, 2005.

[57] R. Niyazov and S. Stepanyan. CLAS-NOTE 2005-021, 2005.

[58] F.-X. Girod and M. Garçon. CLAS-NOTE 2005-001, 2005.

[59] CLAS12 Technical Design Report. http://clasweb.jlab.org/wiki/index.php/CLAS12_Technical_Design_Report, 2008.

[60] M. Ungaro. Clas12 geant-4 simulation package gemc. http://clasweb.jlab.org/wiki/index.php/CLAS12_Software, 2009.

[61] http://clasweb.jlab.org/rungroups/bonus/wiki/index.php/Main_Page, 2004.

[62] http://clasweb.jlab.org/rungroups/lowq/wiki/index.php/Main_Page, 2009.

[63] M. J. M. van Sambeek et al. A recoil detector for the internal target facility of AmPS (NIKHEF). Nucl. Instrum. Meth., A409:443–446, 1998.

[64] K. Assamagan et al. Time-zero fission-fragment detector based on low-pressure multiwire proportional chambers. Nucl. Instrum. Meth., A426:405–419, 1999.

[65] http://www.jlab.org/exp_prog/proposals/06/PR12-06-113.pdf, 2006.